Modelling of pipeline under differential frost heave considering post-peak reduction of uplift resistance in frozen soil

Bipul C. Hawlader, Vincent Morgan, and Jack I. Clark

Abstract: The interaction between buried chilled gas pipelines and the surrounding frozen soil subjected to differential frost heave displacements has been investigated. A simplified semi-analytical solution has been developed considering the post-peak reduction of uplift resistance in frozen soil as observed in laboratory tests. The nonlinear stress–strain behaviour of the pipeline at large strains has been incorporated in the analysis using an equivalent bending stiffness. The predicted results agree well with our finite element analysis and also with numerical predictions available in the literature, hence the simple semi-analytical solution can be considered as an alternative to numerical techniques. A parametric study has been carried out to identify the influence of key factors that can modify the uplift resistance in frozen soil. Among them, the residual uplift resistance has been found to be the important parameter for the development of stresses and strains in the pipeline.

Key words: pipeline, frost heave, discontinuous permafrost, semi-analytical solution, uplift resistance, frozen soil.

Résumé : On a étudié l'interaction entre les pipelines de gaz refroidi et le sol gelé environnant assujettis à des déplacements en soulèvement. On a développé une solution semi-analytique simplifiée en prenant en considération la réduction postpic de la résistance au soulèvement dans le sol gelé telle qu'observée dans les essais en laboratoire. Le comportement contrainte–déformation non linéaire du pipeline à grandes déformations a été incorporé dans l'analyse en utilisant une rigidité équivalente en flexion Les résultats prédits concordent bien avec notre analyse en éléments finis et aussi avec les prédictions numériques disponibles dans la littérature; ainsi, on peut considérer la solution semi-anlytique simple comme étant une alternative aux techniques numériques. On a réalisé une étude paramétrique pour identifier l'influence des facteurs clés qui peuvent modifier la résistance au soulèvement dans le sol gelé. Parmi eux, on a trouvé que la résistance résiduelle au soulèvement était le paramètre important pour le développement des contraintes et des déformations dans le pipeline.

Mots clés : pipeline, soulèvement dû au gel, pergélisol discontinu, solution semi-analytique, résistance au soulèvement, sol gelé.

[Traduit par la Rédaction]

Introduction

The growing interest in northern oil and gas resources demands an efficient design method for arctic pipelines. Pipelines in northern regions are often buried in continuous or discontinuous permafrost and traverse large distances through a variety of soil types in terms of frost susceptibility. The current design philosophy for natural gas pipelines through permafrost is to chill the product to prevent thawing of frozen ground. This causes freezing of initially unfrozen soil when the pipeline passes through unfrozen ground in discontinuous permafrost, however, and results in frost heave induced vertical displacement. Uniform heave is not a major issue for pipeline integrity as long as the minimum cover requirement is maintained; however, differential heave near the interface between two soils with different frost susceptibilities or frozen and unfrozen soil could be a critical issue in designing arctic pipelines. The maximum internal pressure usually dominates the design (wall thickness and grade) of conventional pipelines; however, differential frost heave may be one of the major sources of load for buried chilled pipelines in discontinuous permafrost. The magnitude of frost heave induced stresses and strains in the pipeline depends on the resistance offered by the surrounding soil. For example, a low uplift resistance near the interface could produce a gradual movement of the pipe and therefore generate less frost heave induced stresses and strains (Nixon and Hazen 1993). In a discontinuous permafrost section, the uplift resistance of the frozen (nonheaving) side of the transition is the main concern, as it dominates the design of pipelines based on maximum stress and strain.

The objective of this study is to develop a semi-analytical solution considering the uplift resistance in frozen soil observed in laboratory tests. The main attraction of this approach is that it does not require complex numerical calcula-

Received 15 March 2005. Accepted 16 December 2005. Published on the NRC Research Press Web site at http://cgj.nrc.ca on 10 February 2006.

B.C. Hawlader,[1] V. Morgan, and J.I. Clark. C-CORE, Captain Robert A Bartlett Building, Morrissey Road, St. John's, NL A1B 3X5, Canada.

[1]Corresponding author (e-mail: Bipul.Hawlader@c-core.ca).

 doi:10.1139/T06-003

tions. To verify the solution, the results have been compared with finite difference (Nixon 1994) and finite element results. The effects and sensitivity to several soil parameters are also presented. Although the solution has been developed for differential frost heave, it could also be used for modelling pipelines subjected to transverse soil movements where the post-peak reduction of soil resistance (softening) is a concern.

Past works

The modelling of frost heave induced pipeline–soil interaction is a complex, time-dependent thermo-hydro-mechanical process. The complete coupled analysis of this process is relatively difficult, and therefore in the state of practice two independent analyses are usually performed for frost heave and mechanical response. Many useful concepts relating to frost heave prediction and its implementation for structural analysis of pipelines have been proposed in the past. Considering the pipeline as a passive structural member, Nixon et al. (1983) performed a series of finite element analyses modelling the soil as an elastic and nonlinear viscous continuum. Selvadurai (1988) considered the soil purely as an elastic material. The uplift resistance in frozen soil has been shown to be nonelastic at large displacement (Nixon 1998; Foriero and Ladanyi 1994), and therefore the application of this solution is limited. Shen and Ladanyi (1991) developed a combined numerical algorithm where the heat and moisture movements were simulated using finite difference, and the mechanical behaviour was simulated using the finite element method. Considering elastic, plastic, and creep behaviour of frozen soil, Selvadurai and his co-workers (Selvadurai and Shinde 1993; Selvadurai et al. 1999) presented a more rigorous continuum modelling of pipe–soil interaction. Although continuum modelling provides some advantages, current state of practice uses a beam model where the resistance offered by the surrounding soil is represented by a series of Winkler springs. Several studies using a spring model for frozen soil are available in the literature (e.g., Ladanyi and Lemaire 1984; Rajani and Morgenstern 1993; Nixon 1994; Razaqpur and Wang 1996). One of the key parameters in this type of analysis is the accurate definition of the resistance of the surrounding soil.

Nixon (1998) and Liu et al. (2004) performed a series of midscale laboratory tests to provide uplift resistance functions of frozen soils. It has been shown that the uplift resistance, as a function of pipe displacement, reaches a peak value and then reduces to a residual value at large displacement. Depending on test conditions, the post-peak resistance falls to between 40% and 70% of the peak resistance at a displacement of three times that at the peak resistance and is sensitive to soil temperature, pipe diameter, burial depth, and loading rate. The formation of tension cracks in the frozen soil over and adjacent to the pipe can explain the reduction of this resistance (Nixon 1998; Liu et al. 2004). Foriero and Ladanyi (1994) also performed uplift resistance tests in frozen soil using a 270 mm diameter pipe to understand the mechanism of the full-scale test results from the Caen test facility in France. A similarly shaped uplift resistance function was obtained, although the reduction of resistance after the peak was relatively sharp in comparison to the results of Nixon (1998). Although the mechanism could be different depending on the test conditions and soil type, the shape of the uplift resistance function is similar in all cases. As the tests progressed, the peak resistance developed and was followed by a post-peak reduction of resistance to a residual value at large displacement. Considering the post-peak reduction of uplift resistance in frozen soil, Nixon (1994) developed a numerical algorithm for analyzing pipelines in discontinuous permafrost. It was shown that the predicted bending strain is considerably reduced because of the post-peak reduction of uplift resistance.

For pipelines in northern regions, transitions from frozen to unfrozen frost-susceptible ground can occur several times per kilometre (Greenslade and Nixon 2000). In view of uncertainties in the modelling of frost heave and its effects in the analysis of pipelines in discontinuous permafrost, a simple but sufficiently accurate method of prediction, such as an analytical or semi-analytical solution, would be an efficient method for analyzing pipelines operating under these conditions. Ladanyi and Lemaire (1984) developed a simplified analytical solution considering both soil and pipeline as linear elastic materials. Rajani and Morgenstern (1993) developed an enhanced analytical solution for an elastic pipeline by idealizing the behaviour of frozen soil as an elastic – perfectly plastic material. Major limitations of these solutions are that the uplift resistance in frozen soil has not been modelled as observed in the laboratory (Foriero and Ladanyi 1994; Nixon 1998; Liu et al. 2004), and the nonlinear stress–strain behaviour of the pipeline was not considered.

Soil–pipeline interaction

The soil–pipeline interaction considered in this study is limited to vertical ground movement perpendicular to the pipeline axis. The stress and strain developed in the pipe depend on soil characteristics, pipeline geometry and material properties, and the amount of frost heave experienced. Figure 1 schematically presents an overview of the model used in this study. The free-field frost heave (w_f), where the frost heave is not influenced by the restraint of the pipeline in frozen ground, can be calculated using available frost heave models (Konrad and Morgenstern 1984; Nixon 1986; Shah and Razaqpur 1993; Konrad and Shen 1996; Hawlader et al. 2004). In the same way as described by Rajani and Morgenstern (1992, 1993), it is assumed that the displacement profile of the pipeline due to differential heave follows a double-curvature profile. Also, the process of frost heave in frost-susceptible soil has been decoupled from the mechanical modelling of the pipeline in non-frost-susceptible soil (Rajani and Morgenstern 1993). The action due to frost heave is transferred to the pipeline by applying an end displacement (w_0) at the interface equal to half of the free-field frost heave ($w_f/2$), and the analysis has been carried out only for the portion of the pipeline located in frozen soil. The authors are aware of the fact that the end displacement depends on the coupled process of frost heave and pipeline–soil interaction. The decoupling technique greatly simplifies the analysis, however. Figure 1*b* shows the end displacements for two freezing periods in the Caen large-scale test (Carlson 1994), where an 18 m long pipeline was buried with one half in a frost-susceptible silt and the other half in a non-frost-

Fig. 1. Modelling of differential frost heave. (*a*) Response of pipeline at large end displacement (at intermediate end displacement, $\bar{x}$ = 0; at small end displacement, $x_0 = \bar{x} = 0$). (*b*) Caen full-scale test (data from Carlson 1994). (*c*) Uplift resistance function.

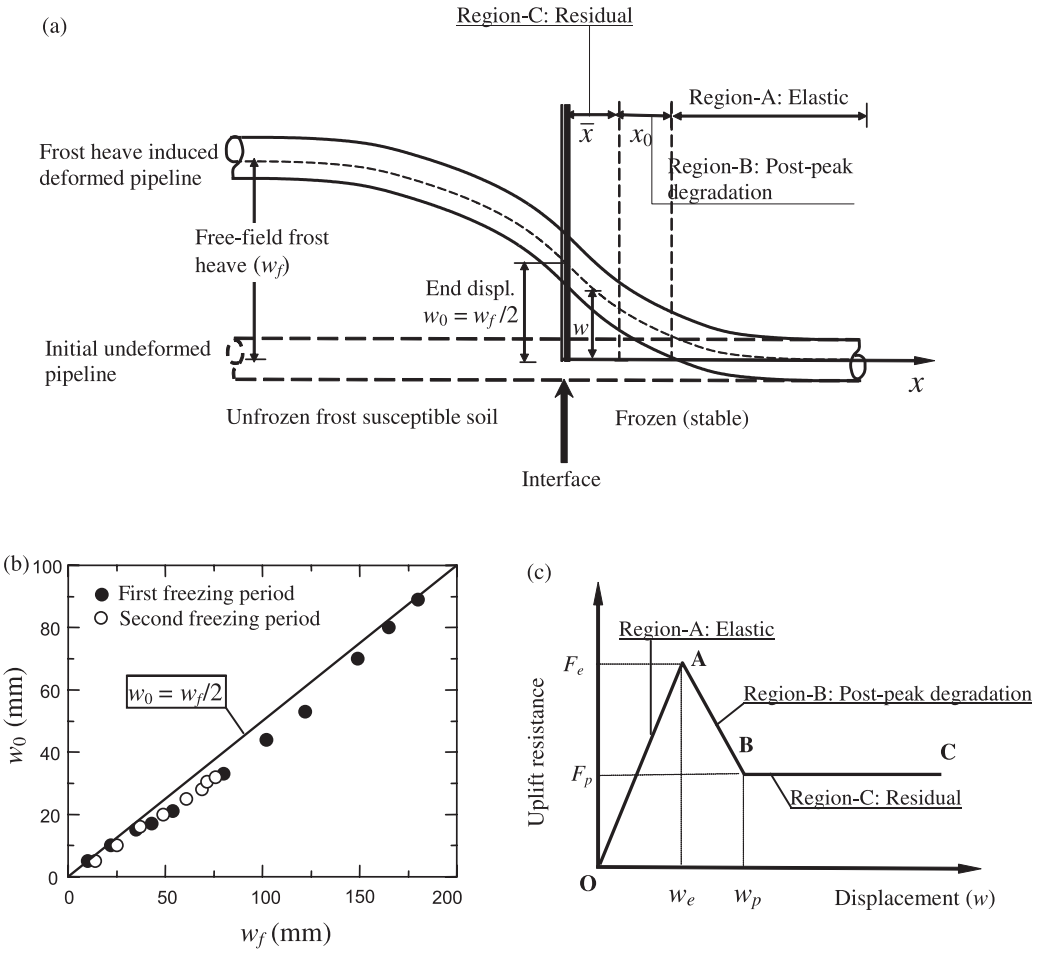

susceptible sand, and the effects of differential frost heave were investigated. In this figure, w_f represents the difference between the vertical displacement of the two ends of the pipe, and w_0 represents the difference between the vertical displacement at the sand–silt interface and the end of the pipe in the non-frost-susceptible sand layer. As shown, measured w_0 is slightly less than $w_f/2$. Therefore, the analyses presented in this study using $w_0 = w_f/2$ will tend to be slightly conservative for this case.

Modelling of soil resistance

The uplift resistance in frozen soil as a function of displacement has been divided into three segments (Fig. 1*c*). The formulation has been performed for three levels of end displacement (small, intermediate, and large) to describe the sequence of deformation during the process of heaving.

At small end displacements ($0 < w_0 \leq w_e$) the upward deformation of soil above the pipeline is essentially elastic, where w_e is the displacement at which the peak uplift resistance (F_e) is developed. The uplift resistance in this range of displacement has been defined using the line OA in Fig. 1*c*, and the segment of the pipe where the surrounding soil behaves elastically has been defined as region A (Fig. 1*a*). At intermediate end displacements ($w_e < w_0 \leq w_p$) the uplift resistance in a segment of the pipe near the interface for a length x_0, where the vertical displacement of the pipe is greater than w_e, decreases from the peak value. This segment has been defined as region B. Here, w_p is the displacement at which the uplift resistance reduces to the residual value (F_p). The uplift resistance in region B has been defined by using the linear line AB shown in Fig. 1*c*. At large end displacements ($w_0 > w_p$) a constant residual uplift resistance (F_p) is developed on a segment of the pipe near the interface which has been defined as region C. The uplift resistance in this region has been defined using the linear line BC in Fig. 1*c*. The horizontal distance from the interface to the point that separates regions B and C is denoted by $\bar{x}$ (Fig. 1*a*).

Mathematical formulation

As three types of uplift resistance are possible depending on the end displacement, the mathematical formulation of these combinations is described separately in the following sections. Note that the displacement (w), slope (ω), bending moment (M), and shear force (S) are always a function of distance (x) along the pipe.

Small end displacement ($0 < w_0 \leq w_e$)

The soil is elastic at this level of end displacement and

only region A is formed. Both x_0 and $\bar{x}$ (Fig. 1*a*) are equal to zero, and the origin is at the interface. The governing differential equation and its solution can be written as (Hetényi 1946)

$$[1] \qquad EI\frac{d^4w_A}{dx^4} + k'_s w_A = 0$$

$$[2] \qquad w_A = \exp(-\beta x)(C_1 \cos \beta x + C_2 \sin \beta x)$$

where EI is the bending stiffness of the pipeline (in which E is the elastic modulus and I is the moment of inertia), w_A is the displacement in region A, C_1 and C_2 are constants, and β is the reciprocal of characteristic length ($= \sqrt[4]{k'_s/4EI}$, where k'_s represents the stiffness of the soil spring). The expressions for slope (ω), bending moment (M), and shear force (S) can be obtained by successive differentiation of eq. [2] and are listed in Appendix A (eqs. [A1]–[A3]).

Imposing boundary conditions at $x = 0$ ($M = 0$ and $w = w_0$), it can be shown that $C_1 = w_0$ and $C_2 = 0$, which have been used to calculate the displacement, slope, bending moment, and shear force using eqs. [2] and [A1]–[A3].

Intermediate end displacement ($w_e < w_0 \le w_p$)

At this level of end displacement the uplift resistance for a length x_0 near the interface is governed by the post-peak degradation line AB (Fig. 1*c*), and the resistance for the rest of the length is still governed by elastic line OA (Fig. 1*c*). Therefore, two segments of uplift resistance function OA and AB define the response of the pipeline in regions A and B, respectively (Fig. 1*a*). Note that $\bar{x} = 0$ at this stage. For mathematical convenience the origin is considered at the point that separates regions A and B. The governing differential equation for region B can be written as

$$[3] \qquad EI\frac{d^4w_B}{dx^4} + k'_s w_B - \alpha k'_s(w_B - w_e) = 0$$

$$\text{with} \qquad \alpha = \frac{k'_s w_p - F_p}{k'_s(w_p - w_e)}$$

where w_B is the displacement in region B. The factor α (>1) defines the rate of degradation of uplift resistance after the peak: the higher the value of α, the faster the rate of degradation. Note that α equals 0 and 1 represent elastic and elastic – perfectly plastic conditions, respectively. Equation [3] can be rewritten as

$$[4] \qquad \frac{d^4w_B}{dx^4} - \frac{k'_s(\alpha - 1)}{EI} w_B + \frac{\alpha k'_s w_e}{EI} = 0$$

The solution of this differential equation is

$$[5] \qquad w_B = \alpha w_e/(\alpha - 1) + C_3 \cos \mu x + C_4 \sin \mu x + C_5 \cosh \mu x + C_6 \sinh \mu x$$

where $\mu = \sqrt[4]{k'_s(\alpha - 1)/EI}$, and C_3–C_6 are unknown constants. Again, the expressions for slope, bending moment, and shear force can be obtained by successive differentiation of eq. [5] and are listed in Appendix A (eqs. [A4]–[A6]).

The governing differential equation and its solution for region A are the same as eqs. [1] and [2], respectively. Note that eq. [2] also represents the elastic behaviour for small end displacements, but the boundary conditions for obtaining the constants C_1 and C_2 are different. The following boundary conditions should be used to obtain the constants (C_1–C_6 and x_0) for intermediate end displacement.

Boundary conditions

At $x = -x_0$, the displacement and bending moment are equal to w_0 and zero, respectively. Therefore, using eqs. [5] and [A5] we have

$$[6] \qquad C_3 \cos \mu x_0 - C_4 \sin \mu x_0 + C_5 \cosh \mu x_0 - C_6 \sinh \mu x_0 = w_0 + \alpha w_e/(1 - \alpha)$$

$$[7] \qquad -C_3 \cos \mu x_0 + C_4 \sin \mu x_0 + C_5 \cosh \mu x_0 - C_6 \sinh \mu x_0 = 0$$

Considering the displacement and slope compatibility and the moment and shear force equilibrium at $x = 0$, the following relationships can be obtained:

$$[8] \qquad C_3 + C_5 - C_1 = \alpha w_e/(1 - \alpha)$$

$$[9] \qquad C_4 + C_6 = \psi[-C_1 + C_2] \qquad \text{where } \beta/\mu = \psi$$

$$[10] \qquad -C_3 + C_5 = -2\psi^2 C_2$$

$$[11] \qquad -C_4 + C_6 = 2\psi^3[C_1 + C_2]$$

Lastly, the rate of shear force variation, $EI(d^4w_A/dx^4)$, at $x = 0$ is equal to the peak soil resistance (F_e), which yields

$$[12] \qquad C_1 = F_e/4\beta^4 EI$$

Equations [8]–[12] have been used to obtain the unknown constants (C_1–C_6 and x_0). A simple solution procedure has been described in Appendix B. Once the values of these constants are known, the variation of displacement, slope, bending moment, and shear force can be calculated using eqs. [2], [5], and [A1]–[A6].

Large end displacement ($w_0 > w_p$)

When the end displacement (w_0) is greater than w_p, the constant residual uplift resistance (F_p) will be developed on a portion of the pipe near the interface (region C in Fig. 1*a*) where the displacement of the pipe exceeds w_p. Next to this region, where the displacement of the pipe is more than w_e but less than w_p, there will be another region B where the post-peak degradation line AB (Fig. 1*c*) represents the uplift resistance. The uplift resistance on the rest of the pipe (region A) is still governed by elastic soil deformation. For mathematical convenience, the origin is considered at the point that separates regions B and C.

The governing differential equation and its solution for region C ($-\bar{x} \le x \le 0$) can be written as

$$[13] \qquad EI\frac{d^4w_C}{dx^4} = -F_p$$

$$[14] \qquad w_C = -\frac{F_p x^4}{24EI} + C_7\frac{x^3}{6} + C_8\frac{x^2}{2} + C_9 x + C_{10}$$

where w_C is the displacement in region C. Once again, the expressions for slope, bending moment, and shear force can be obtained by successive differentiation of eq. [14] and are listed in Appendix A (eqs. [A7]–[A9]).

The displacements for region A ($x > x_0$) and region B ($0 < x \le x_0$) are given in eqs. [2] and [5], respectively, although the boundary conditions for obtaining C_1–C_6 are different from those described for small and intermediate end displacements.

Boundary conditions

At $x = -\bar{x}$, the displacement and bending moment are equal to w_0 and zero, respectively. Now, using eqs. [14] and [A8] we have

$$[15] \quad -\frac{F_p \bar{x}^4}{24EI} - C_7 \frac{\bar{x}^3}{6} + C_8 \frac{\bar{x}^2}{2} - C_9 \bar{x} + C_{10} - w_0 = 0$$

$$[16] \quad C_8 = \frac{\bar{x}[F_p \bar{x} + 2C_7 EI)]}{2EI}$$

Now, considering the displacement and slope compatibility and the moment and shear force equilibrium at $x = 0$ and $x = x_0$, the following relationships can be obtained:

$$[17] \quad C_{10} = -[\alpha w_e/(1 - \alpha)] + C_3 + C_5$$

$$[18] \quad C_9 = \mu(C_4 + C_6)$$

$$[19] \quad -C_3 + C_5 = C_8/\mu^2$$

$$[20] \quad C_7 = \mu^3(-C_4 + C_6)$$

$$[21] \quad -[\alpha w_0/(1 - \alpha)] + C_3 m_1 + C_4 m_2 + C_5 m_3 + C_6 m_4 = C_1 b_1 + C_2 b_2$$

$$[22] \quad -m_2 C_3 + m_1 C_4 - m_4 C_5 + m_3 C_6 = \psi[C_1(-b_2 - b_1) + C_2(-b_2 + b_1)]$$

$$[23] \quad -C_3 m_1 + C_4 m_2 + C_5 m_3 - C_6 m_4 = 2\psi^2[C_1 b_2 - C_2 b_1]$$

$$[24] \quad m_2 C_3 - m_1 C_4 + m_4 C_5 + m_3 C_6 = 2\psi^3[C_1(b_1 - b_2) + C_2(b_2 + b_1)]$$

where $m_1 = \cos \mu x_0$, $m_2 = \sin \mu x_0$, $m_3 = \cosh \mu x_0$, $m_4 = \sin \mu x_0$, $b_1 = \exp(-\beta x_0) \cos \beta x_0$, and $b_2 = \exp(-\beta x_0) \sin \beta x_0$.

Lastly, the rate of shear force variation at $x = 0$ and $x = x_0$ is equal to F_p and F_e, respectively, which yields

$$[25] \quad C_3 + C_5 = -F_p/\mu^4 EI$$

$$[26] \quad C_1 = \{F_0/[4\beta^4 EI \exp(-\beta x_0)\cos \beta x_0]\} - C_2 \tan \beta x_0$$

Equations [15]–[26] have been used to obtain the unknown constants (C_1–C_{10}, x_0, and $\bar{x}$). A simple solution procedure has been described in Appendix C. Once the values of these constants are known, the variation of displacement, slope, bending moment, and shear force along the length of the pipe can be calculated using eqs. [2], [5], [14], and [A1]–[A9].

Fig. 2. Moment–curvature relationship for steel pipeline used in the analysis.

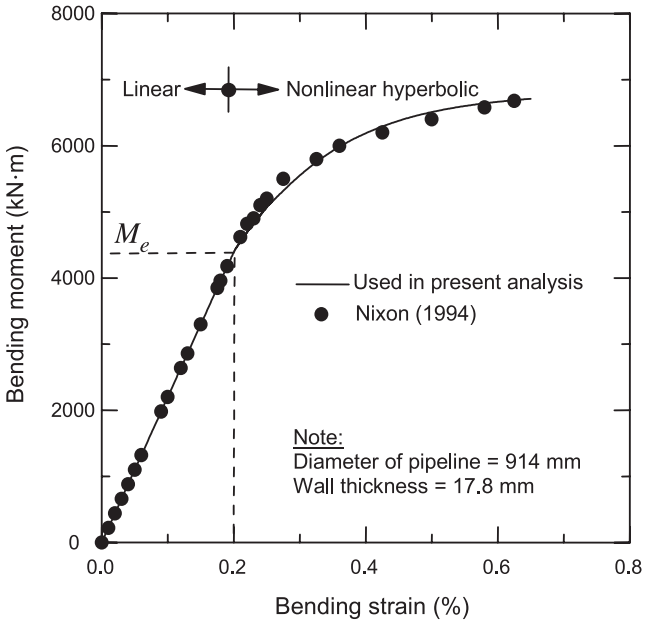

Nonlinear behaviour of pipeline

Large differential movement of the pipeline due to frost heave may generate strains greater than the linear elastic limit of the pipe material. The strain at the linear elastic limit is about 0.1% for mild steel and up to 0.25% for higher strength steels often used for high-pressure oil and gas pipelines (Prevost 1995). Figure 2 shows the moment–curvature relationship used in this study, where the linear elastic limit is at 0.2% strain. The response until 0.2% strain has been modelled using a linear elastic modulus, E = 204 GPa. The nonlinear behaviour after this linear elastic limit (0.2%) has been defined using a hyperbolic relationship as shown in Fig. 2. The calculation has been limited to the allowable strain limit of 0.5% (Canadian Standards Association 2003), however.

Cubrinovski and Ishihara (2004) proposed a simplified method for modelling the nonlinear behaviour of piles based on the maximum bending moment. It was shown that their simplified method slightly overpredicts the maximum bending moment beyond the linear elastic limit. A similar approach with some modification to control the overprediction of bending moment has been used in this study. The maximum moment (M_{max}) along the length of the pipe is calculated for each increment. If M_{max} is greater than the linear elastic bending moment (M_e) (Fig. 2), the average bending moment M_{av} (= $(M_{max} + M_e)/2$) has been calculated. Now using the moment–curvature relationship defined in Fig. 2, the strain (ε) required to generate this moment has been obtained and then the equivalent stiffness ($EI_{eq} = M_{av}D/2\varepsilon$, where D is the diameter of the pipe) has been calculated. The elastic bending moment has been used as a reference because this represents the critical moment after which nonlinearity starts. The equivalent stiffness based on M_{max} and M_e provides a reasonable estimate of the average bending stiffness for modelling nonlinear behaviour (Cubrinovski and Ishihara

2004). Note that EI_{eq} obtained from this method is less than the value obtained using Cubrinovski and Ishihara and therefore reduces overprediction of bending moment. If M_{max} is less than M_e, initial bending stiffness should be used.

It should be noted that the solution has been obtained by imposing incremental end displacement, as the behaviour of both soil and pipeline are nonlinear. The calculation has been performed at each step based on the level of end displacement as described in the section entitled "Mathematical formulation", and the corresponding bending stiffness has been updated.

Verification of semi-analytical solution

Nixon (1994) numerically modelled the effects of frost heave on a pipeline in discontinuous permafrost. The diameter and wall thickness of the pipeline were 914 and 17.8 mm, respectively. To demonstrate the accuracy of the present semi-analytical solution, a pipeline having the same geometry and material properties has been considered. Figure 2 shows the moment–curvature relationship of the pipeline as used in Nixon. The uplift resistance of the frozen soil has been modelled using the values presented by Nixon (see inset to Fig. 3*a*). The peak uplift resistance is 585 kN/m at a displacement of 25 mm, which subsequently reduces to one half (292.5 kN/m) at a displacement of 50 mm. The uplift resistance is constant (292.5 kN/m) beyond 50 mm of displacement. The other parameters used in this analysis are listed in Table 1. Note that the analysis using this condition is referred to as the baseline analysis in the following sections. Nixon also calculated 900 mm of free-field frost heave (w_f) after 10 years of chilled pipeline operation, which is equivalent to 450 mm (= 900/2 mm) of end displacement (w_0) in this study.

Figures 3*a* and 3*b* show the predicted bending moment and soil reaction on the pipeline using the present semi-analytical solution. Nixon's (1994) numerical predictions in the nonheaving side are also shown for comparison. The predicted bending moment using the semi-analytical solution is very close to the numerical prediction except near the interface, which is the consequence of using the double-curvature assumption in this analysis. The magnitude and location of the maximum bending moment are of primary interest in pipeline design for these conditions, which are almost identical in both solutions. Once the bending moment is known, the bending strain can be calculated using the moment–curvature relationship shown in Fig. 2. A comparison between the predicted bending strain using the semi-analytical solution and Nixon's numerical prediction is shown in Fig. 3*c*. Both methods predict similar bending strain, indicating that the simple semi-analytical solution could be used for the analysis of pipelines in discontinuous permafrost.

It has been shown that an equivalent stiffness (EI_{eq}) has been used in the semi-analytical solution when the bending moment is greater than M_e. To examine the accuracy of the prediction using EI_{eq}, a rigorous nonlinear finite element analysis has been performed using ABAQUS/Standard-6.3 finite element (FE) code. The interaction between the pipeline and surrounding soil has been modelled using two-dimensional pipe–soil interaction elements (PSI24). The nonlinear behaviour of the pipeline, shown in Fig. 2, has been incorporated in the FE analysis. The uplift resistance (inset to Fig. 4*a*) has also been specified as a function of relative displacement. Figure 4 shows the response of the pipe-

Fig. 3. Comparison between semi-analytical solution and numerical analysis (free-field frost heave w_f = 900 mm).

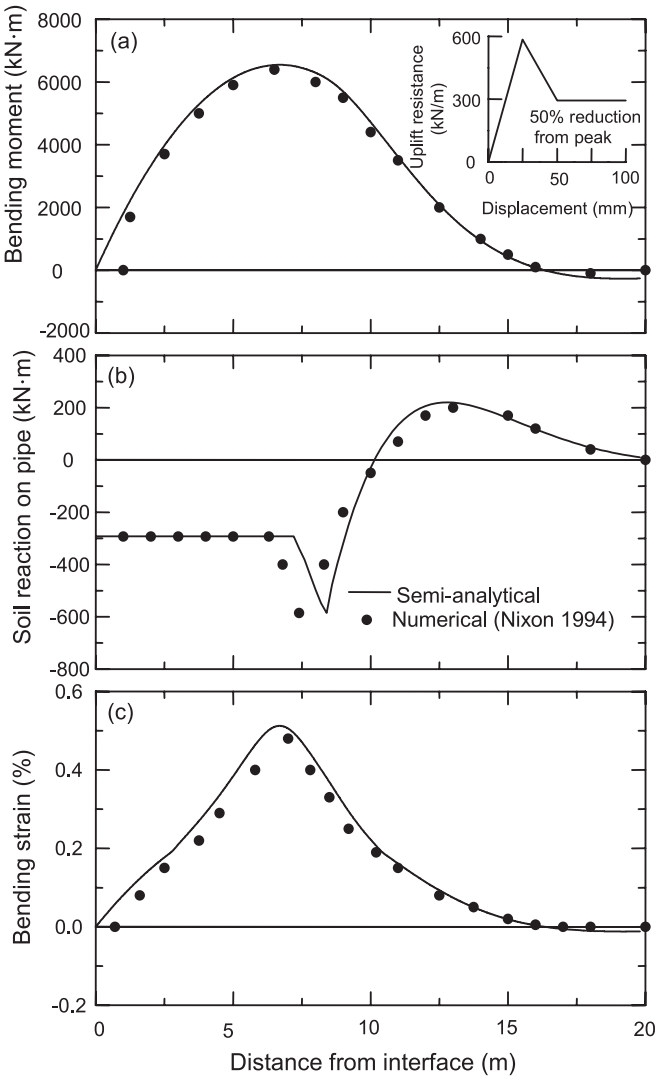

Table 1. Geometry and parameters used for baseline analysis.

Pipeline geometry	
Diameter of pipeline, D (mm)	914
Wall thickness, t (mm)	17.8
Soil properties	
Peak uplift resistance, F_e (kN/m)	585
Displacement at peak resistance, w_e (mm)	25
Residual uplift resistance, F_p (kN/m)	292.5
Displacement at residual resistance, w_p (mm)	50
Soil stiffness before the peak, $k'_s = (F_e/w_e)$ (MPa)	23.4
Resistance reduction factor, α	1.5
Pipeline material properties	
Elastic modulus, E (GPa)	204
Linear elastic strain limit (%)	0.2

Fig. 4. Comparison between semi-analytical solution and finite element (FE) analysis (free-field frost heave w_f = 400 and 900 mm).

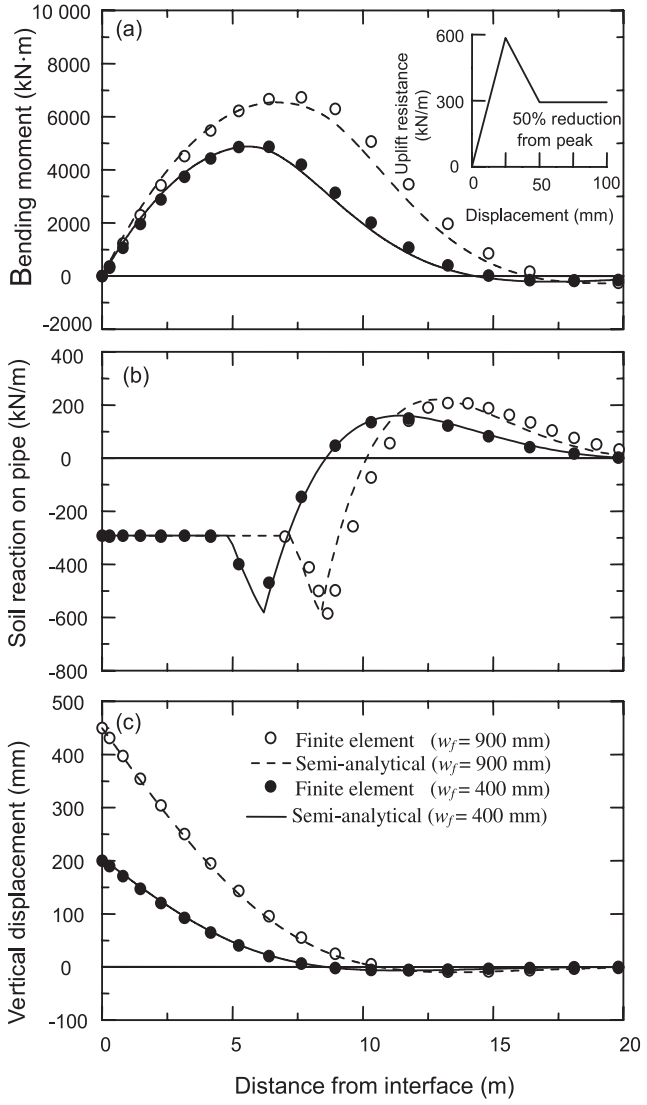

line for two different levels of end displacement. Very good agreement has been found for predicted displacement, soil reaction, and bending moment using both solutions.

To account for the effects of nonlinear deformation of the pipeline, Rajani et al. (1995) suggested an approximate method using an equivalent stiffness (E_sI) based on a secant modulus of elasticity $E_s = \sigma_y/0.005$, where σ_y is the yield stress and 0.005 (= 0.5%) is the allowable longitudinal stain limit for steel pipeline design (Canadian Standards Association 2003). As the modulus of elasticity of steel used in this analysis is 204 GPa, the yield stress (σ_y) is 408 MPa at 0.2% strain. Therefore, the equivalent secant modulus of elasticity (E_s) is calculated to be 81.6 GPa. Using this equivalent stiffness (E_sI) and keeping other parameters the same, the semi-analytical solution is used to predict the response of the pipeline. Figure 5 shows the development of maximum bending moment with heave. The approximate method using E_sI (Rajani et al. 1995) predicts less moment than the present study. It is worth noting that the structural design of arctic pipelines must satisfy the requirements for both hydraulic and frost-heave load. If hydraulic requirements (hoop stress) govern the design and the frost-heave displacement is relatively low but sufficient to produce bending strain more than the linear elastic limit (0.2%), then it is possible that the maximum strain along the length of the pipe never reaches close to 0.5%. In that case, E_sI underestimates equivalent stiffness and predicts lower bending moment.

Fig. 5. Predicted maximum bending moment versus heave.

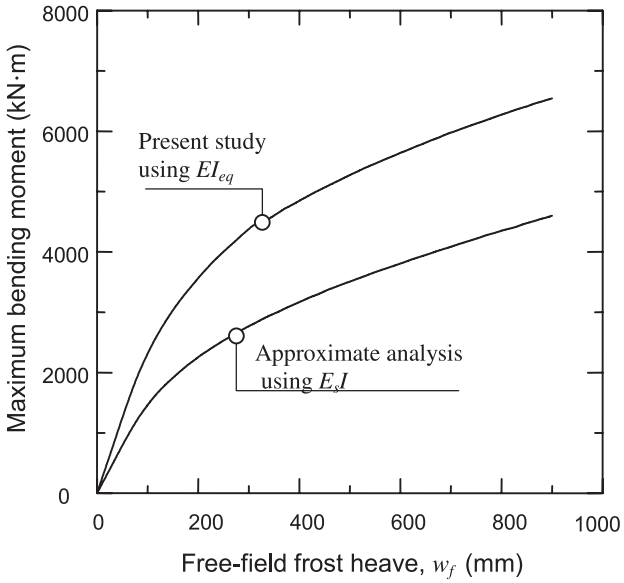

Parametric study

Laboratory tests (Foriero and Ladanyi 1994; Nixon 1998; Liu et al. 2004) show that the uplift resistance in frozen soil varies widely as a function of conditions such as soil type, temperature, and loading rate. Therefore, a parametric study using the present semi-analytical solution has been performed to gain some insight into the effects of some factors on the response of the pipeline. The parametric study has been carried out by varying one parameter at a time while keeping all other parameters at the same value as that of the baseline analysis (Table 1).

Post-peak reduction of uplift resistance

Nixon (1998) and Liu et al. (2004) reported a wide variation of post-peak reduction of uplift resistance. Figure 6 shows the prediction using four different values (0%, 25%, 50%, and 75%) of post-peak reductions (see inset to Fig. 6*a*). Figure 6*a* shows the development of the maximum bending moment with heave displacement until the maximum bending strain exceeds the allowable strain limit (0.5%). The initial linear increase in moment is due to the fact that both soil and pipeline are elastic at this level of heave. Beyond this, a nonlinear increase in bending moment occurs as the soil resistance moves to post-peak resistance in a segment of the pipe near the interface. The increase in bending moment is further reduced at higher heave because at this level of displacement the bending strain in the pipeline exceeds the linear elastic limit (0.2%) and follows the nonlinear hyperbolic relationship (Fig. 2). It can be also seen

Fig. 6. Effects of post-peak reduction. (*a*) Maximum moment versus heave. (*b*, *c*) Variation of bending moment and soil reaction versus distance from interface for w_f = 500 mm.

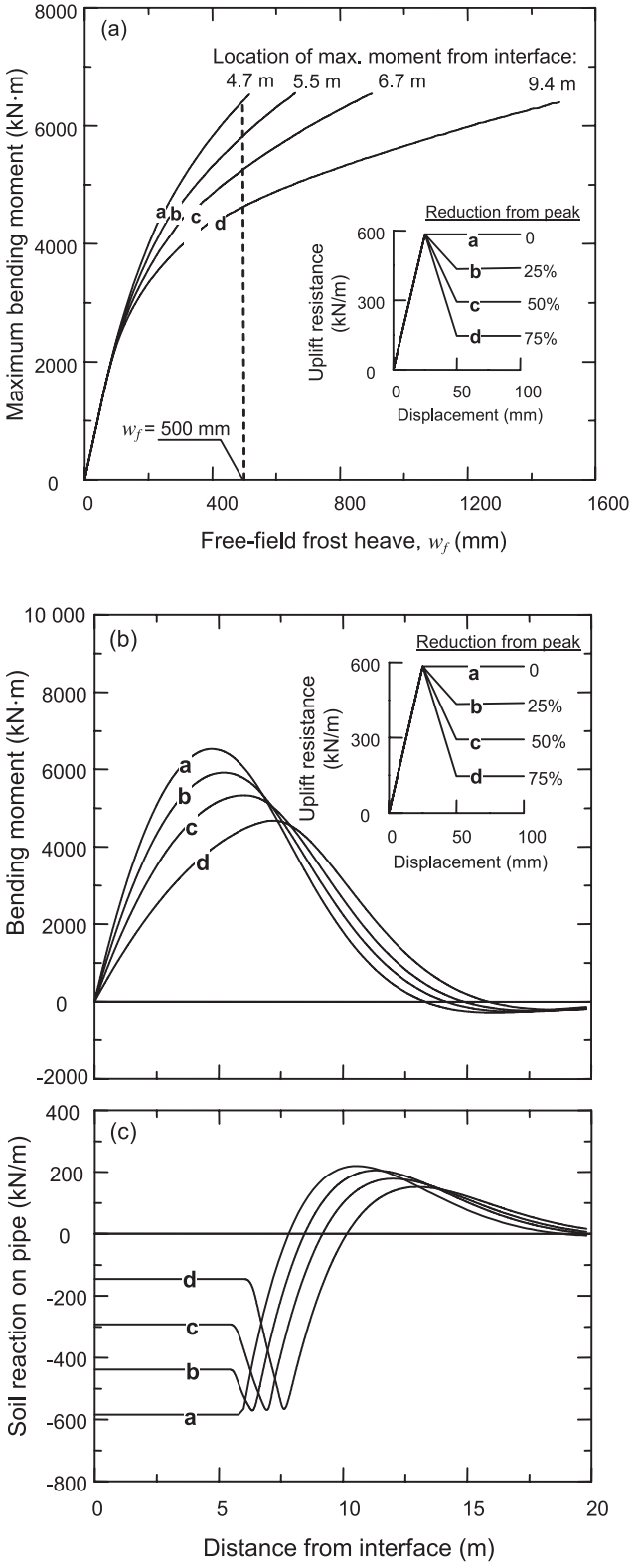

from Fig. 6*a* that, when the reduction of uplift resistance is considered, the designer can allow greater heave displacement before reaching the allowable strain limit. For example, the pipeline can sustain only 500 mm of free-field frost heave if no post-peak reduction is considered, whereas the same pipeline can sustain 900 mm of free-field frost heave when 50% reduction of post-peak resistance is allowed. The location of the maximum bending moment at the onset of 0.5% strain limit is shown at the end of each curve in Fig. 6*a*. As shown, the location of the maximum bending moment moves farther away from the interface with decreasing residual resistance.

The effects of post-peak reduction for a given end displacement are shown in Figs. 6*b* and 6*c*. A value of 500 mm of free-field frost heave has been used for this comparison. As shown, the predicted bending moment is significantly higher if post-peak reduction is not considered. Moreover, the location of the maximum bending moment moves farther from the interface with higher post-peak reduction of uplift resistance.

Rate of post-peak degradation

Experimental results (Foriero and Ladanyi 1994; Nixon 1998) show that the displacement required for post-peak reduction of uplift resistance varies widely depending on the test conditions. To investigate the effects of this reduction rate, three cases have been considered (inset to Fig. 7*a*). In each case the peak uplift resistance is developed at 25 mm of displacement, followed by the reduction of resistance to a residual value of 50% of the peak at 50 mm, 75 mm, and 100 mm. The bending moment and soil reaction on the pipeline at 900 mm of free-field frost heave are shown in Figs. 7*a* and 7*b*, respectively. Although there is a little variation of soil resistance on the pipeline (Fig. 7*b*), the variation of bending moment is negligible. This implies that the effect of post-peak reduction rate is less significant at this level of displacement. Although the predicted bending moment using these degradation rates is very close at 900 mm of heave, this is not always the case during the whole process of heave. As shown in Fig. 7*c*, there is some difference in predicted bending moment at a lower level of heave, for example at 300 mm of free-field frost heave. This difference is not significant compared with the effects of other factors, however.

Initial stiffness of soil spring

Many uncertainties exist about the soil spring stiffness, although it is an important parameter in regular pipeline design (Kruisman and Radder 1990; Zhou and Murray 1993). Therefore, the design codes suggest that the effect of varying this parameter should be checked. For example, Dutch pipeline rules suggest that this effect should be checked by varying the stiffness using a factor of 1.4 on the mean value (divide by 1.4 for a lower bound value and multiply by 1.4 for an upper bound value). To investigate the effects of soil stiffness, three different stiffness values have been considered as shown in the inset to Fig. 8*a*. In each case, the peak resistance is assumed to be developed at 25 mm, and a constant residual resistance of 292.5 kN/m is developed at 50 mm. The initial stiffness of cases a and c, respectively, is 1.5 times lower and 1.5 times higher than that of the baseline analysis (case b). Figures 8*a* and 8*b* show the variation of bending moment and soil reaction along the length of the pipe at 900 mm of free-field frost heave. As shown in

Fig. 7. Effects of post-peak reduction rate. (*a*, *b*) Variation of bending moment and soil reaction versus distance from interface for w_f = 900 mm. (*c*) Maximum moment versus heave.

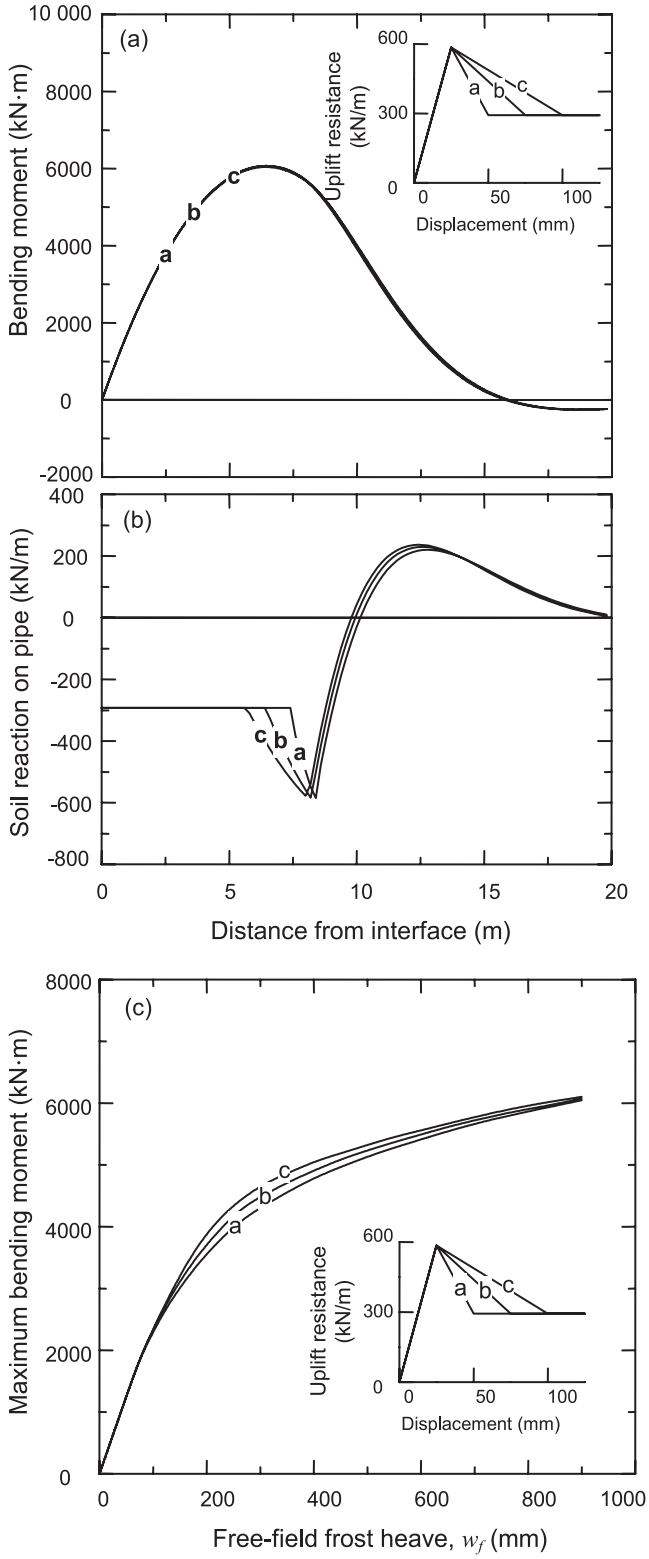

Fig. 8. Effects of initial soil stiffness. (*a*, *b*) Variation of bending moment and soil reaction versus distance from interface for w_f = 900 mm. (*c*) Maximum moment versus heave.

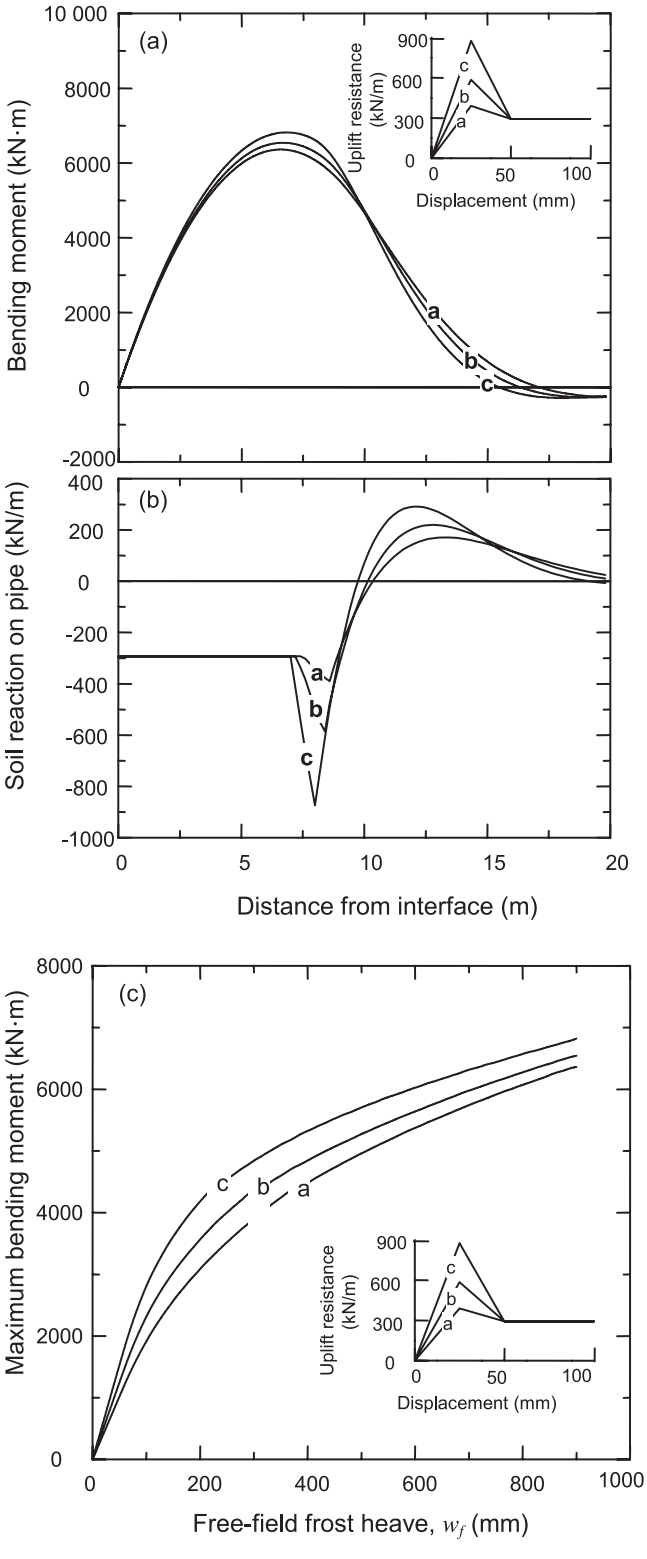

Fig. 8*a*, the maximum bending moment is increased slightly by the increase in initial stiffness. The maximum bending moment is not as close for these three cases during the whole process of heaving, as shown in Fig. 8*c*. For example, the maximum bending moment for case c is only 7% higher than that for case a at 900 mm of free-field frost heave,

whereas it is 35% higher at 200 mm of free-field frost heave. This suggests that the initial soil stiffness has a significant effect at small to intermediate heave displacements but smaller effects at large displacements.

Conclusions

A semi-analytical solution has been presented for the analysis of a pipeline subjected to differential frost heave displacement. The post-peak reduction of uplift resistance in frozen soil has been incorporated in the analysis. The nonlinear stress–strain behaviour of the pipeline has been modelled using an equivalent bending stiffness based on the maximum bending moment and linear elastic bending moment. A very good agreement has been found between the present semi-analytical solution and numerical predictions. The semi-analytical solution has also been used to perform a parametric study to identify the effects of key variables, which control the uplift resistance function, on the response of a pipeline subjected to differential heave. Based on this study, the following conclusions are drawn:

(1) The post-peak reduction of uplift resistance in frozen soil has a significant effect on the frost-heave-induced bending moment. The residual resistance at large displacement is one of the critical design parameters.
(2) The rate of post-peak reduction of uplift resistance has minimal influence for the range considered in this study.
(3) The soil stiffness before the peak has a significant effect at small to intermediate levels of heave displacement; however, its effect is less significant at large heave displacement.
(4) The proposed equivalent bending stiffness method can be used for modelling the nonlinear behaviour of pipelines.

Although the present study provides a quick and efficient method of prediction considering only the mechanical aspects of the pipeline in the frozen ground, the analysis will not be valid for some special cases such as a pipeline crossing through a short section of unfrozen ground. In this case, a complete numerical modelling of the pipeline in both frozen and unfrozen sections is required. One of the major sources of error in any semi-analytical or numerical prediction, however, is the definition of the uplift resistance in frozen soil, which is a complex function of temperature, pipe diameter, burial depth, and loading rate (Nixon 1998).

Acknowledgements

The work presented in this paper was funded internally by C-CORE with support from the Pipeline Research Council International (PRCI) and the Gas Technology Institute (GTI). The authors express their sincerest thanks to Dr. Kenny, Senior Manager Pipelines at C-CORE, for his valuable suggestions.

References

Canadian Standards Association. 2003. Oil and gas pipeline systems. Standard CSA Z662-03, Canadian Standards Association, Rexdale, Ont.

Carlson, L. 1994. Database report for the Caen Frost Heave Testing Facility. Report for National Energy Board, Engineering Branch, L.E.C. Engineering, Calgary, Alta.

Cubrinovski, M., and Ishihara, K. 2004. Simplified method for analysis of piles undergoing lateral spreading in liquefied soils. Soils and Foundations, **44**: 119–134.

Foriero, A., and Ladanyi, B. 1994. Pipe uplift resistance in frozen soil and comparison with measurements. Journal of Cold Regions Engineering, ASCE, **8**: 93–111.

Greenslade, J.G., and Nixon, J.F. 2000. New design concepts for pipelines buried in permafrost. *In* Proceedings of the International Pipeline Conference 2000, Calgary, Alta., 1–5 October 2000. American Society of Mechanical Engineers (ASME), New York. Vol. 1, pp. 135–144.

Hawlader, B.C., Morgan, V., and Clark, J.I. 2004. A simplified solution for frost heave prediction of chilled pipelines. *In* Cold Regions Engineering, Proceedings of the 12th International Specialty Conference, Edmonton, Alta., 16–19 May 2004. American Society of Civil Engineers, New York. Paper 127. 8 pp.

Hetényi, M. 1946. Beams on elastic foundation. University of Michigan Press, Ann Arbor, Mich. 255 pp.

Konrad, J.-M., and Morgenstern, N.R. 1984. Frost heave prediction of chilled pipelines buried in unfrozen soils. Canadian Geotechnical Journal, **21**: 100–115.

Konrad, J.-M., and Shen, M. 1996. 2-D frost heave action model using segregation potential of soils. Cold Regions Science and Technology, **24**: 263–278.

Kruisman, G., and Radder, K.W. 1990. Influence of the soil in advanced buried pipeline flexibility analysis. *In* Proceedings of the Pipeline Technology Conference, Oostende, Belgium, 15–18 October 1990. *Edited by* R. Denys. KVIV, Ghent, Belgium. pp. 12.1–12.12.

Ladanyi, B., and Lemaire, G. 1984. Behaviour of a buried pipeline under differential frost heave conditions. *In* Cold Regions Engineering, Proceedings of the 3rd International Specialty Conference, Montréal, QC, 4–6 April 1984. *Edited by* D.W. Smith. Canadian Society for Civil Engineering, Montréal, Que. pp. 161–176.

Liu, B., Crooks, J., Nixon, J.F., and Zhou, J. 2004. Experimental studies of pipeline uplift resistance in frozen soil. *In* Proceedings of the International Pipeline Conference, IPC 2004, Calgary, AB, 4–8 October 2004. American Society of Mechanical Engineers, New York. Paper IPC04-0133. 7 pp.

Nixon, J.F. 1986. Pipeline frost heave predictions using a 2-D thermal model. *In* Research on Transportation Facilities in Cold Regions, Proceedings of a Session in Conjunction with the ASCE Convention, Boston, Mass. American Society of Civil Engineers, New York. pp. 67–82.

Nixon, J.F. 1994. Role of heave pressure dependency and soil creep stress analysis for pipeline frost heave. *In* Cold Regions Engineering, Proceedings of the 7th International Specialty Conference, Edmonton, Alta., 7–9 March 1994. *Edited by* D.W. Smith and D.C. Sego. Canadian Society for Civil Engineering, Montréal, Que. pp. 397–412.

Nixon, J.F. 1998. Pipe uplift resistance testing in frozen soil. *In* Proceedings of the 7th International Conference on Permafrost, Yellowknife, NT, 23–27 June 1998. *Edited by* A.G. Lewkowicz and M. Allard. Université Laval, Nordicana Collection No. 57. pp. 821–831.

Nixon, J.F., and Hazen, B. 1993. Uplift resistance of pipelines buried in frozen ground. *In* Proceedings of the 6th International Conference on Permafrost, Beijing, China. South China University of Technology Press, Wushan, Guangzhou, China. Vol. 1, pp. 494–499.

Nixon, J.F., Morgenstern, N.R., and Reesor, S.N. 1983. Frost heave – pipeline interaction using continuum mechanics. Canadian Geotechnical Journal, **20**: 251–261.

Prevost, R.C. 1995. Strain equation. Incidence on buried steel pipe design. *In* Proceedings of the 2nd International Conference on Advances in Underground Pipeline Engineering, Bellevue, Wash., 25–28 June 1995. *Edited by* J.K. Jeyapalan and M. Jeyapalan. American Society of Civil Engineers, New York. pp. 394–405.

Rajani, B., and Morgenstern, N. 1992. Behaviour of a semi-infinite beam in a creeping medium. Canadian Geotechnical Journal, **29**: 779–788.

Rajani, B., and Morgenstern N. 1993. Pipelines and laterally loaded piles in an elastoplastic medium. Journal of Geotechnical Engineering, ASCE, **119**: 1431–1448.

Rajani, B.B., Robertson, P.K., and Morgenstern, N.R. 1995. Simplified design methods for pipelines subject to transverse and longitudinal soil movements. Canadian Geotechnical Journal, **32**: 309–323.

Razaqpur, A.G., and Wang, D. 1996. Frost-induced deformations and stresses in pipelines. International Journal of Pressure Vessels and Piping, **69**: 105–118.

Selvadurai, A.P.S. 1988. Mechanics of soil–pipeline interaction. *In* Proceedings of the Annual Conference, Calgary, Alta., 23–27 May 1988. Canadian Society for Civil Engineering, Montréal, Que. pp. 151–173.

Selvadurai, A.P.S., and Shinde, S.B. 1993. Frost heave induced mechanics of buried pipelines. Journal of Geotechnical Engineering, ASCE, **119**: 1929–1951.

Selvadurai, A.P.S., Hu, J., and Konuk, I. 1999. Computational modelling of frost heave induced soil-pipeline interaction II. Modelling of experiments at the Caen Test Facility. Cold Regions Science and Technology, **29**: 229–257.

Shah, K.R., and Razaqpur, A.G. 1993. A two-dimensional frost heave model for buried pipelines. International Journal for Numerical Methods in Engineering. **36**: 2545–2566.

Shen, M., and Ladanyi, G. 1991. Soil–pipe interaction during frost heaving around a buried chilled pipeline. *In* Cold Regions Engineering, Proceedings of the 6th International Specialty Conference, West Lebanon, NH, 26–28 February 1991. *Edited by* D.S. Sodhi. American Society of Civil Engineers, New York. pp. 11–21.

Zhou, Z., and Murray, D.W. 1993. Behaviour of buried pipelines subjected to imposed deformation. *In* Proceedings of the 12th International Conference on Offshore Mechanics and Arctic Engineering, Pipeline Technology, Glasgow, Scotland, 20–24 June 1993. American Society of Mechanical Engineers, New York. Vol. 5, pp. 115–122.

List of symbols

C_1–C_{10}	constants
D	diameter of pipeline
E	elastic modulus of pipeline
E_s	secant modulus of elasticity
EI	bending stiffness
EI_{eq}	equivalent stiffness
F_e	peak resistance
F_p	residual resistance
I	moment of inertia
k'_s	soil stiffness before the peak (= F_e/w_e)
M	bending moment, $f(x)$
M_{av}	average bending moment
M_e	elastic bending moment
M_{max}	maximum moment
S	shear force, $f(x)$
t	wall thickness
w	displacement, $f(x)$
w_A, w_B, w_C	displacement in regions A, B, and C
w_e	displacement at peak resistance
w_f	free-field frost heave
w_p	displacement at residual resistance
w_0	vertical displacement at the interface (= $w_f/2$)
x	distance along the pipeline
x_0	pipe segment where post-peak degradation occurs
$\bar{x}$	horizontal distance from the interface to the point that separates regions B and C
α	resistance reduction factor
β	reciprocal of characteristic length
ε	strain
μ	constant
σ_y	yield stress
ω	slope, $f(x)$

Appendix A: Expressions for slope (ω), bending moment (M), and shear force (S)

Region A

$$[A1]\quad \omega_A = \frac{dw_A}{dx} = \beta \exp(-\beta x)[C_1(-\sin\beta x - \cos\beta x) + C_2(-\sin\beta x + \cos\beta x)]$$

$$[A2]\quad M_A = -EI\frac{d^2w_A}{dx^2} = -2EI\beta^2 \exp(-\beta x)[C_1 \sin\beta x - C_2 \cos\beta x]$$

$$[A3]\quad S_A = -EI\frac{d^3w_A}{dx^3} = -2EI\beta^3 \exp(-\beta x)[C_1(\cos\beta x - \sin\beta x) + (C_2 \sin\beta x + \cos\beta x)]$$

Region B

$$[A4]\quad \omega_B = \frac{dw_B}{dx} = \mu(-C_3 \sin\mu x + C_4 \cos\mu x + C_5 \sinh\mu x + C_6 \cosh\mu x)$$

$$[A5]\quad M_B = -EI\frac{d^2w_B}{dx^2} = -EI\mu^2(-C_3 \cos\mu x - C_4 \sin\mu x + C_5 \cosh\mu x + C_6 \sinh\mu x)$$

$$[A6]\quad S_B = -EI\frac{d^3w_B}{dx^3} = -EI\mu^3(C_3 \sin\mu x - C_4 \cos\mu x + C_5 \sinh\mu x + C_6 \cosh\mu x)$$

Region C

$$[A7] \quad \omega_C = \frac{dw_C}{dx} = -\frac{F_p x^3}{6EI} + C_7 \frac{x^2}{2} + C_8 x + C_9$$

$$[A8] \quad M_C = -EI \frac{d^2 w_C}{dx^2} = F_p \frac{x^2}{2} - EI(C_7 x + C_8)$$

$$[A9] \quad S_C = -EI \frac{d^3 w_C}{dx^3} = F_p x - EIC_7$$

Appendix B: Solution for the constants at intermediate end displacement ($w_e \le w_0 \le w_p$)

Using eqs. [8]–[11], the expressions for C_3–C_6 in terms of C_2 have been obtained as follows:

$$[B1] \quad C_3 = \frac{v_1}{2} + \psi^2 C_2$$

$$[B2] \quad C_4 = \frac{(-\psi - 2\psi^3)}{2} v_0 + \frac{\psi - 2\psi^3}{2} C_2$$

$$[B3] \quad C_5 = \frac{v_1}{2} - \psi^2 C_2$$

$$[B4] \quad C_6 = \frac{(-\psi + 2\psi^3)}{2} v_0 + \frac{\psi + 2\psi^3}{2} C_2$$

Now, inserting these expressions into eq. [7] gives

$$[B5] \quad C_2 = \frac{v_1 \cos \mu x_0 + (\psi + 2\psi^3) \sin \mu x_0 - v_1 \cosh \mu x_0 - (\psi - 2\psi^3) \sin \mu x_0}{-2\psi^2 \cos \mu x_0 + (\psi - 2\psi^3) \sin \mu x_0 - 2\psi^2 \cosh \mu x_0 - (\psi + 2\psi^3) \sinh \mu x_0}$$

where $v_0 = F_e/4\beta^4 EI$, and $v_1 = F_e/4\beta^4 EI + \alpha w_e/(1 - \alpha)$.

Using the remaining boundary condition (eq. [6]) for a trial and error approach, the unknown constants (C_1–C_6 and x_0) have been obtained. For a given value of x_0, calculate C_2 using eq. [B5] and then obtain the values of C_3–C_6 using eqs. [B1]–[B4]. Now check whether it satisfies eq. [6]; if it does not, update the value of x_0 based on the simple bisection method.

Appendix C: Solution for the constants at large end displacement ($w_0 > w_p$)

Inserting ($C_3 + C_5$) from eq. [25] into eq. [17] gives

$$[C1] \quad C_{10} = -\frac{\alpha w_e}{(1 - \alpha)} - \frac{F_p}{\mu^4 EI}$$

Using eqs. [19] and [25], we have

$$[C2] \quad C_3 = -\frac{F_p}{2\mu^4 EI} - \frac{C_8}{2\mu^2}$$

and

$$[C3] \quad C_5 = -\frac{F_p}{2\mu^4 EI} + \frac{C_8}{2\mu^2}$$

As the equations obtained from the boundary conditions (eqs. [15]–[26]) are not linear, the following trail and error approach has been used to solve these equations for unknowns:

(1) Set the values of C_4, C_6, $\bar{x}$, and x_0. The first trial starts with their values in the previous step.
(2) Calculate C_7 (eq. [20]), C_8 (eq. [16]), C_9 (eq. [18]), C_{10} (eq. [C1]), C_3 (eq. [C2]), and C_5 (eq. [C3]).
(3) Check whether it satisfies eq. [15]. If not, increase or decrease the value of $\bar{x}$ depending on a negative or positive value of the left-hand side of eq. [15]. Repeat steps 2 and 3 until it becomes within the limit of tolerance. Using the calculated values of C_3 and C_5 and replacing C_1 using eq. [26], calculate the values of C_2, C_4, and C_6 using eqs. [22]–[24].
(4) Check whether it satisfies eq. [21]. If not, update the value of x_0 and repeat steps 4 and 5 until it satisfies the desired level of tolerance.
(5) Update the values of C_4 and C_6 as the averages of their assumed and calculated values, and repeat the calculation until the difference between the calculated values of unknowns in two successive trials is within the limit of tolerance.